Polar Biol
DOI 10.1007/s00300-013-1311-y

ORIGINAL PAPER

Testate amoebae and environmental features of polygon tundra in the Indigirka lowland (East Siberia)

A. A. Bobrov · S. Wetterich · F. Beermann ·
A. Schneider · L. Kokhanova · L. Schirrmeister ·
L. A. Pestryakova · U. Herzschuh

Received: 30 May 2012 / Revised: 22 February 2013 / Accepted: 24 February 2013

Abstract Polygon tundra characterizes large areas of arctic lowlands. The micro-relief pattern within polygons offers differentiated habitats for testate amoeba (testacean) communities. The objective of this study was to relate testacean species distribution within a polygon to the environmental setting. Therefore, testaceans from four cryosol pits dug at different locations within a low-centered polygon were studied in the context of pedological and pedochemical data, while ground temperature and ground moisture were measured over one summer season. The study site is located on the Berelekh River floodplain (Indigirka lowland, East Siberia). The environmental data sets reflect variations along the rim-to-center transect of the polygon and in different horizons of each pit. The testacean species distribution is mainly controlled by the soil moisture regime and pH. Most of the identified testaceans are cosmopolitans; eight species are described from an arctic environment for the first time. Differences in environmental conditions are controlled by the micro-relief of polygon tundra and must be considered in arctic lowland testacean research because they bias species composition and any further (paleo-)ecological interpretation.

Keywords Arctic tundra · Permafrost · East Siberia · Testaceans · Cryosols · Patterned ground

Introduction

The testate amoebae (Protozoa: Testacealobosea and Testaceafilosea; testaceans) are a group of free-living protozoans that have an organic shell (testa). Testaceans inhabit practically all water and land habitats, but abundance and diversity are usually highest in peatlands and in the litter of coarse, humus-rich soils. Testate amoebae, being inherently aquatic, restructure their communities in response to environmental changes in, for example, ground-water table, soil moisture, pH, content of biophilic elements (N, P, K, Ca, Mg), and organic matter (Gilbert et al. 1998; Wilkinson and Mitchell 2010). Due to their indicator potential, testaceans have been extensively applied in paleoecological research (e.g., Charman 2001; Charman et al. 2007; Mitchell et al. 2008; Lamarre et al. 2012; Payne et al. 2006, 2012). Sphagnobiontic species serve as reliable model organisms because they react distinctly to changes in light, soil temperature, soil moisture, and oxygen concentration (Mitchell and Gilbert 2004). Testacean communities preserved in permafrost are increasingly employed to reconstruct local soil conditions during the late Quaternary past (Bobrov et al. 2004, 2009; Andreev et al. 2009; Müller et al. 2009; Meyer et al. 2010; Schirrmeister et al. 2011; Wetterich et al.

Electronic supplementary material The online version of this article (doi:10.1007/s00300-013-1311-y) contains supplementary material, which is available to authorized users.

A. A. Bobrov · L. Kokhanova · U. Herzschuh
Department of Soil Science, Moscow State University,
Vorobievy Gory, 119991 Moscow, Russia

S. Wetterich (✉) · A. Schneider · L. Schirrmeister
Department of Periglacial Research, Alfred Wegener Institute
for Polar and Marine Research, Telegrafenberg A43,
14473 Potsdam, Germany
e-mail: sebastian.wetterich@awi.de

F. Beermann
Institute of Soil Science, University of Hamburg,
Allende-Platz 2, 20146 Hamburg, Germany

L. A. Pestryakova
Department for Geography and Biology, Northeastern Federal
University of Yakutsk, ul. Belinskogo 58, 677000 Yakutsk,
Russia

2012), while modern testate amoeba research in tundra environments focuses on using testaceans as indicators of ongoing climate warming processes in the terrestrial Arctic (Beyens et al. 2009; Tsyganov et al. 2011, 2012).

Polygonal tundra patterned-ground elements are sensitive indicators of environmental and climate changes. Polygon ponds, mires, and cryosols are typical components of arctic Siberian wetlands underlain by permafrost. Recently, testaceans from modern tundra habitats have been described from several arctic and subarctic regions in Greenland, Canada, Sweden, and Alaska (Beyens et al. 1986a, b, 1990, 1992; Beyens and Chardez 1995; Trappeniers et al. 1999; Beyens et al. 2000; Mattheeussen et al. 2005; Payne et al. 2006; Markel et al. 2010). These studies focused on surface samples. Testacean species abundance and diversity along a depth gradient in soil profiles and spatial distribution within, for example, a polygon structure have not been studied in the Arctic, although Vincke et al. (2006) examined species distribution from subantarctic soil profiles.

In most organic-rich permafrost soils, vertical stratification reflects different stages of organic turnover or humification of floral, faunal, and microbial remains. Each soil horizon represents a distinct ecological niche for its resident testate amoeba species. Therefore, the polygon micro-relief controlling, for example, the vegetation cover and the moisture content as well as the depth at which testaceans occur below the surface have great importance for testacean studies in tundra soils. The moisture regime in arctic soils underlain by permafrost is triggered by the seasonal (summertime) thawing of the uppermost layer and the waterlogging of this active layer above the impermeable permafrost table by precipitation and melt-water. These characteristics have not been taken into account in testacean studies of arctic environments to date.

The study presented here aims to (1) determine temporal and spatial variations of environmental parameters affecting testate amoeba communities in arctic polygon tundra; (2) differentiate testate amoeba habitats within the polygon micro-relief; and (3) estimate the most important control on testacean species distribution. Besides producing an inventory and achieving a deeper ecological understanding of arctic testaceans, such research leads to improved interpretation of fossil testate amoeba communities from permafrost deposits.

The fieldwork was undertaken in the summer of 2011 (Schirrmeister et al. 2012). This study contributes to the understanding of arctic polygonal landscape functioning and dynamics in a changing Arctic. Biotic assemblages and abiotic parameters in polygons were studied to deduce modern environmental conditions in polygonal landscapes. In this context, the testate amoeba response to variation in the abiotic environmental parameters which generate spatial polygon structures was of special interest.

Present assemblages of testate amoebae were collected and their occurrence was compared with on-site measured meteorological, hydrological, pedological, and pedochemical data.

Materials and methods

Study site

The study area was located in the floodplain and the adjacent thermokarst-affected lowland along the Berelekh River, a tributary of the Indigirka River, 28 km northwest of the settlement of Chokurdakh near the Kytalyk WWF (World Wildlife Fund) station (70°83′12.1N, 147°48′29.9E; Fig. 1). The Berelekh River is well known in Quaternary research because of the Berelekh “mammoth graveyard” that exists upstream of the river (e.g., Pitulko 2011).

The vegetation is described as a tussock-sedge, dwarf shrub, moss tundra (CAVM Team 2003). The climate is continental, characterized by high annual temperature amplitudes and low precipitation. According to meteorological data from the closest station in Chokurdakh [World Meteorological Organization (WMO) station no. 21946], the mean air temperature of the warmest month (T_{July}) is +9.7 °C and that of the coldest month (T_{January}) is −36.6 °C. The mean annual air temperature (T_{Ann}) is −14.2 °C, while the mean annual precipitation ($\mathrm{P}_{\mathrm{Ann}}$) does not exceed 350 mm (Rivas-Martinez 1996–2009). The region belongs to the continuous permafrost zone; only the uppermost decimeters thaw seasonally during summer to form the active layer. The perennially frozen ground is between 200 and 300 m deep, and ground temperature is between −6 and −4 °C (Geocryological Map 1991).

The modern relief is characterized by late Pleistocene Ice Complex (Yedoma) remnant hills up to several decameters high which are intersected by extensive basins (Alas) 15 km and more in diameter. The basins formed due to permafrost thawing and subsequent surface subsidence (i.e., thermokarst) during warm stages, including the present Holocene. Such thermokarst (Alas) basins are often occupied by water bodies (thermokarst lakes) which are surrounded by polygonal frost-crack systems. In some places, the Berelekh River has cut through Alas basins which are situated 4–6 m above river level. The KYT-1 polygon study site was located in the southernmost part of an Alas basin that is drained by the Konsor-Syane River, which flows from north to south through the entire Alas and discharges into the Berelekh River. Polygonal structures within the Alas average 20 × 20 m. The development of modern ice wedges and the resulting polygonal patterned relief is obvious. Low-centered polygons are commonly seen due to their distinct rims which delineate the underlying ice-wedge systems.

Fig. 1 Location of the Kytalyk study site in the northeastern Siberian lowland. DEM prepared by G. Grosse (University of Alaska Fairbanks)

Fieldwork

The KYT-1 study site is a typical low-centered polygon about 20 m in diameter located on the upper Alas level. Polygon walls and frost cracks enclose it completely. A monitoring station was established and the environmental data were collected between July 19 and August 27, 2011 (Fig. 2). We installed ground temperature sensors in the polygon rim (T1) and center (T2), and soil moisture sensors (M) in the rim slope at different depths (Table 1). The air temperature (Ta) was measured at a height of 2 m above the rim. All data loggers recorded values every 30 min to provide high resolution.

On August 26, 2011, at the end of the field season, active-layer and ground surface measurements were carried out along a 21-m-long SE–NW transect across the KYT-1 polygon with the 1-m resolution (Figs. 2, 3). To obtain data about the surface micro-relief and to establish a horizontal reference line above the transect, we used a so-called water level tube. A flexible tube with open ends was filled with water. Based on the position of the meniscus in the tube, we could construct a horizontal line, which was indicated using a string attached every 3 m to a wooden pole. We measured the ground surface elevation, the water table height, and the active-layer depth and performed a simplified vegetation survey across the polygon. Four soil pits (pits 1–4; Fig. S1) were dug within the active layer of the KYT-1 polygon down to the permafrost table; one profile was located on the polygon rim (pit 1), one on the inner slope (pit 2), and two in the center (pits 3 and 4; Fig. 2). The description of the soil types follows the US soil taxonomy (Soil Survey Staff 2010) and the Russian soil classification (Shishov et al. 2004). At each profile, one surface (vegetation) sample was collected and three soil samples (each about 100 g) were taken from distinct horizons for further pedochemical and testate amoeba analyses. The vegetation was sampled in 0.5 × 0.5 m plots. For estimating the cover and the species abundance, the Braun-Blanquet scale, modified by Reichelt and Willmanns (1973), was used.

Chemical analyses (pH, electrical conductivity, nutrients, C, N, C/N) and water content

Electrical conductivity (EC) and pH were measured by a portable measuring device (WTW, pH/Cond 340i). The water content of fresh soil samples was measured gravimetrically after drying in an oven. To assess the pools of available nutrients, ammonium, nitrate, and phosphate were measured. Both investigated nitrogen compounds were extracted by a 0.0125-M $CaCl_2$ solution (VDLUFA 1991). This extraction removes only plant-available molecules. Phosphate was measured by extraction with 0.5-M $NaHCO_3$ solution (Ivanoff et al. 1998). This method allows the pool of phosphorus which can be mobilized during one growing season to be estimated (Bowman and Cole 1978).

Fig. 2 Overview of the monitoring setup in polygon KYT-1. The studied soil pits within polygon KYT-1 are labeled as pit 1 (*rim*), pit 2 (*inner slope*), pit 3 (*center*), and pit 4 (*center*). The A-to-B transect across the polygon refers to Fig. 3 where ground surface elevation data and active-layer depth are shown

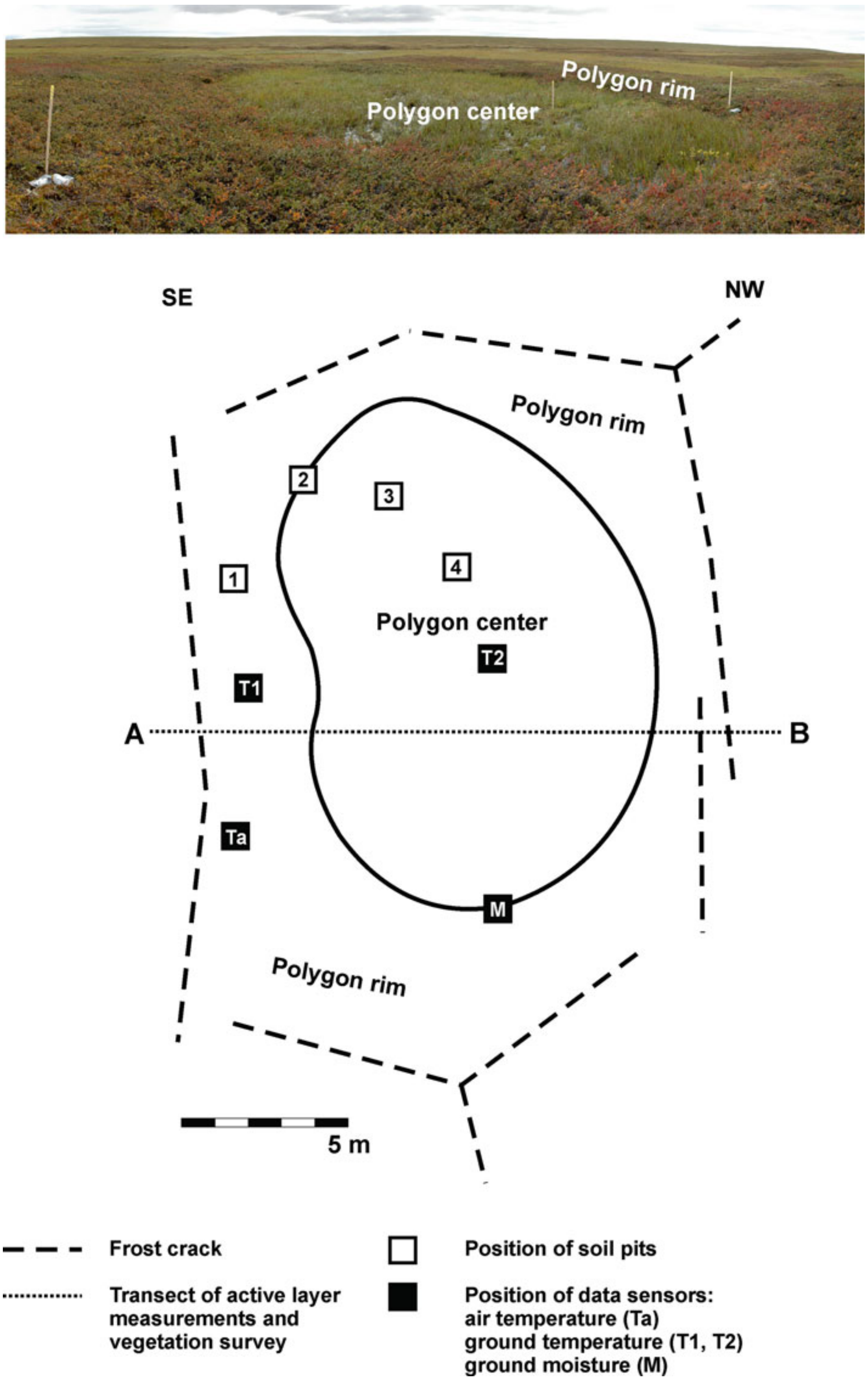

Table 1 Overview of installed data sensor locations, logger types, and time periods

Parameter	Location	Device	Measuring period
Ground temperature (T1)	Polygon rim at depths of: 5, 10, 15, 20 cm	HOBO 12-Bit T smart sensor	19/07/11–27/08/11
Ground temperature (T2)	Polygon center at depths of: 10, 15, 20, 30 cm	HOBO 12-Bit T smart sensor	19/07/11–27/08/11
Air temperature (Ta)	2 m above ground	MinidanTemp 0.1 ESYS	20/07/11–27/08/11
Soil moisture (M)	Polygon inner slope at depths of: 12, 22, 27, 30 cm	HOBO soil moisture smart sensor	19/07/11–27/08/11

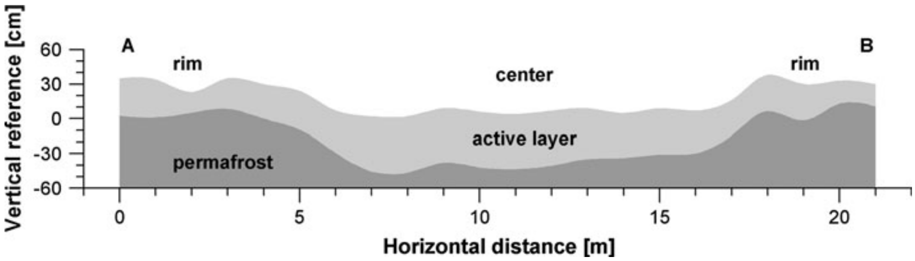

Fig. 3 Ground surface elevation and active-layer depth along the A-to-B transect of polygon KYT-1 on August 26, 2011

The amounts of nutrients in these extracts were photometrically measured with a portable photometer (Hach Lange, DR 2800) and test kits for rapid chemical analysis (Hach Lange, LCK 304 ammonium, LCK 339 nitrate, LCK 349 phosphate). Values are given as NO_3–N, NH_4–N, and PO_4–P.

For the analyses of total carbon and nitrogen, a subsample was ground to <0.06 mm with a vibration disc mill (Conrad TS 100) and dried at 105 °C in a drying oven. For carbon and nitrogen detection by means of a CN analyzer (Vario Max Elementar), a fine-ground sample between 0.3 and 0.7 g, depending on the amount of organic matter, was combusted at 900 °C with oxygen (DIN 1996). The total organic carbon content could be used for calculating the C/N ratio because organic matter dominated in the studied soil pits.

Testate amoeba analysis

For testate amoeba analysis, in total 16 subsamples (from each horizon in each soil pit) of about 3 g were first suspended in distilled water and passed through a 0.5-mm meshed sieve to remove large masking organic and mineral particles. Then, a drop of suspension mixed with a drop of glycerin was placed on a glass slide. Testaceans were identified and counted under light microscope at 100× to 400× magnifications (Zeiss Axioskop 2). On average, five slides were examined for each sample.

Multivariate statistics

The lowermost samples of each plot (Bg horizon) were excluded from statistical analyses due to scarcity or lack of testate amoebae. A non-metric multidimensional scaling (nMDS, $k = 2$; Bray-Curtis as dissimilarity measure) was applied to the square-root transformed and Wisconsin double-standardized percentage data to visualize the main structure of the data set. The soil properties (C, N, C/N, water content, depth [cm]) and sample location (horizon [1–upper, 2–middle, 3–lower], "proximity to rim" [1–distant center, 2–proximal center, 3–inner slope, 4–rim]) were superimposed on the data set. Analyses were performed using the R software (R Development Core Team 2008) "vegan" package (Oksanen et al. 2008).

Results

Vegetation

The vegetation of the investigated polygon was divided into two vegetation types. The vegetation of the polygon rim was dominated by dwarf shrubs (*Betula nana*), herbs (*Ledum palustre*, *Vaccinium vitis-idaea*), and mosses (*Aulacomnium palustre*, *Hylocomium splendens*). The vegetation of the wet polygon center was characterized by sedges (*Carex stans*, *Carex chordorhizza*, *Eriophorum angustifolium*) and herbaceous species (*Potentilla palustris*).

Active-layer depth

The active-layer depth, that is, the seasonally thawed uppermost layer between the ground surface and the permafrost table, was estimated across the KYT-1 polygon at the very end of the field season in order to obtain the data when maximum depths were expected. The mean active layer of the rim was about 27 cm (ranging from 18 to 32.5 cm); this is somewhat shallower than in the polygon center where the mean active-layer depth was about 43 cm (ranging from 33.5 to 48.5 cm; Fig. 3).

Monitoring data (air temperatures, soil temperatures, soil moisture)

The recorded air and ground temperatures of the upper horizons show similar patterns although the daily amplitudes of air temperature patterns are much higher (Fig. 4). A general cooling trend toward the end of the summer season is obvious. The ground temperatures of the lower horizons (below 20 cm depth) were less affected by day-to-day air temperature variations; due to the shallow permafrost table, fairly stable temperatures between 0 and 4 °C were observed. Compared to the record from the polygon rim (T1), the thermal differentiation in the polygon center (T2) is more distinct, and the temperature range is wider in the lower horizons. The volumetric water content data measured by the soil moisture sensors on the polygon inner slope (M) do not exhibit a significant pattern during the observed period; they show a largely constant moisture

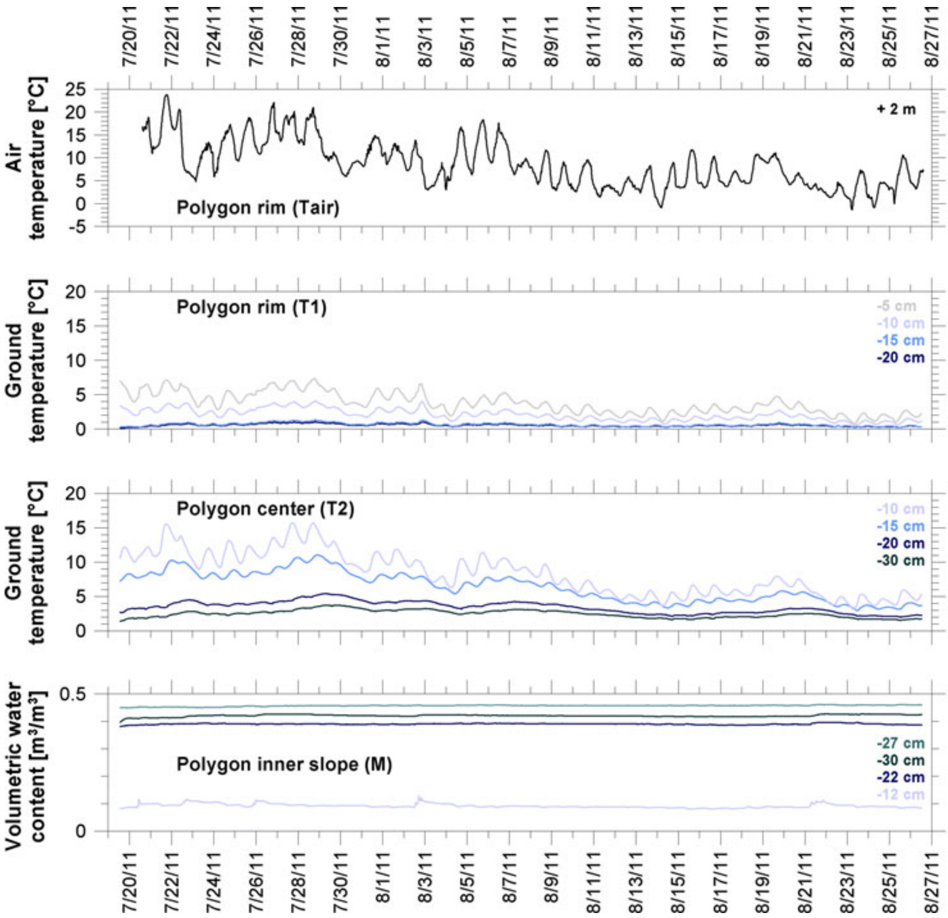

Fig. 4 Air and ground temperatures and soil moisture (volumetric water content) measured in the KYT-1 polygon wall and in the polygon center from July 19 until August 26, 2011

distribution within the active layer. The uppermost sensor at 12-cm depth indicates the driest conditions of about 0.07–0.09 m^3/m^3 volumetric water content, interrupted by some short-term rainfall events which are reflected by volumetric water content that abruptly increased to 0.128 m^3/m^3. Such events also registered as a weaker signal in the deeper sections. The highest moisture content of 0.44–0.46 m^3/m^3 was recorded by the second-lowest sensor 27 cm below the surface, while the lowermost sensor located right above the permafrost table, 30 cm below the surface, measured a slightly lower volumetric water content of 0.39–0.43 m^3/m^3.

Soil profiles

The studied soils of polygon KYT-1 (Fig. S1) belong to Histel subgroups (Histic Gelisols; Soil Survey Staff 2010) or Peaty Gley soils (Shishov et al. 2004); these are permafrost soils with high organic matter content. A further differentiation was carried out by examining the different decomposition states of the organic material and the occurrence of underlying ice layers. Soils on the polygon rim above recent ice wedges were classified as Typic Glacistel (US) or Peaty Gley soil (Russian). The center of polygon KYT-1 consisted of Typic Sapristel (US) or Humic Peaty Gley soil (Russian). Such soils are composed of three horizons, including two peat horizons in different decomposition states (Oi, Oe (US) and T0, T1 (Russian)) and a lowermost mineral horizon above the permafrost table (Bg (US) and G (Russian)).

Chemical properties of soils and water content

The soils in the KYT-1 polygon were moderately acidic (pH 4.0–5.3) and the pH mostly increased with depth (Fig. 5). The EC was remarkably higher on the polygon rim than in the center. The water content decreased toward the permafrost table in each pit and increased from the rim toward the center, reaching 85 %. The lowest nutrient values were always found in the mineral horizon. The highest concentrations of nitrogen and of extractable ammonium were identified in the subsurface horizon (Oe). Carbon concentrations and extractable nitrate and phosphate decreased with depth in each pit. Higher C/N ratios of up to 28 occurred in the Oi horizons of the better drained rim and decreased toward the center to about 19.

Fig. 5 Pedochemical parameters in polygon KYT-1

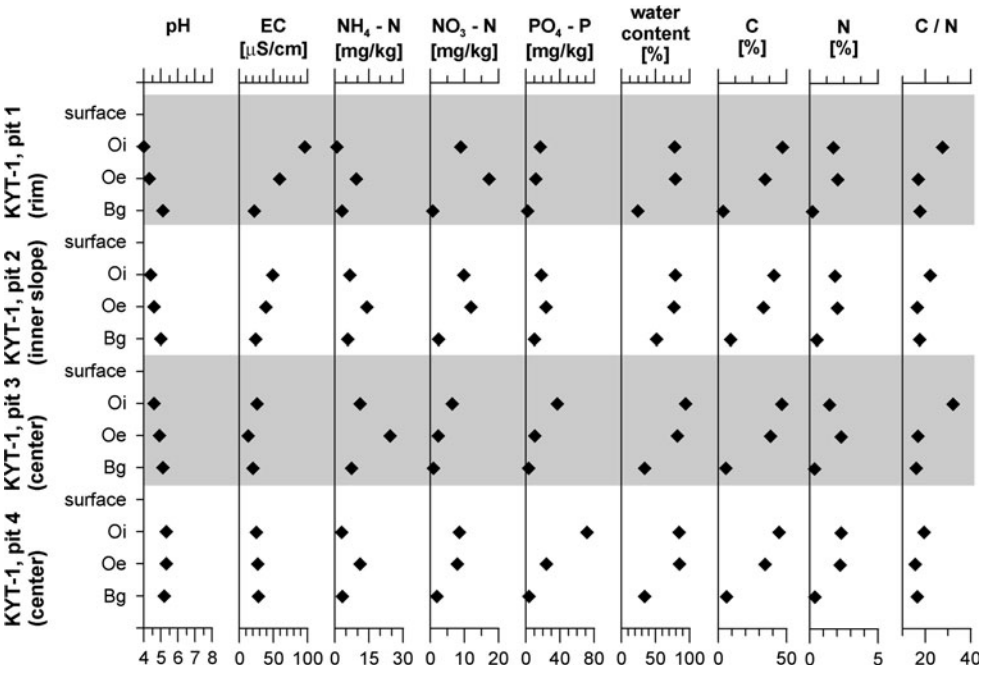

Fig. 6 The nMDS biplot indicates the relationship of the taxa and samples of the rhizopod data set from four sections (pit 1, 2, 3, 4) sampled at three horizons (S, Oi, Oe) of polygon KYT 1. Supplementary environmental variables were superimposed on the plot

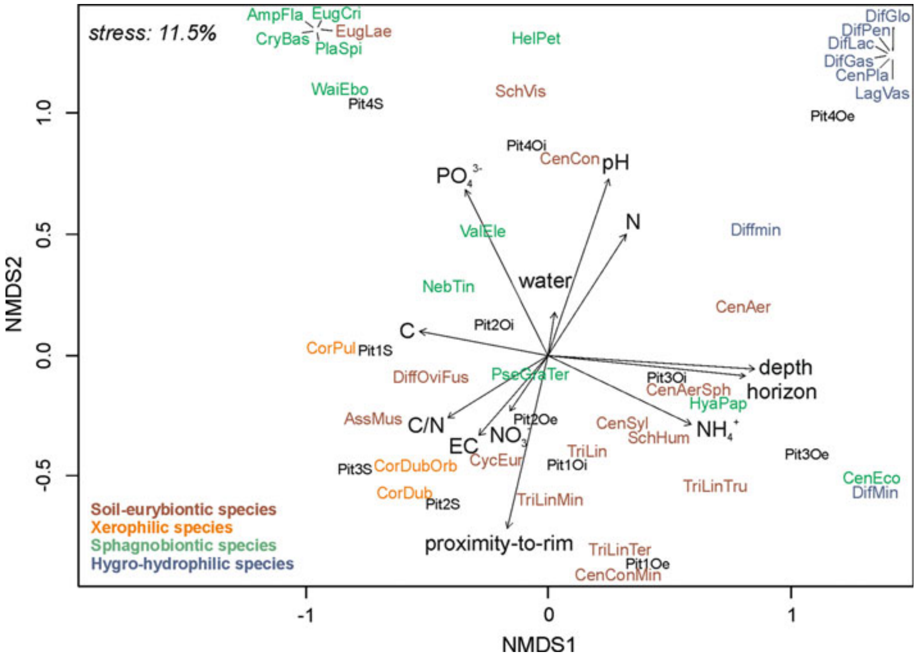

Testate amoeba species distribution

A total of 37 testacean taxa of 19 genera were identified in 16 samples from four pits in polygon KYT-1 (Fig. 6; Table 2). The following species have been found in three or more samples: *Trinema lineare*, *Difflugiella oviformis* f. *fusca*, *Cyclopyxis eurystoma*, *Assulina muscorum*, *Centropyxis constricta*, *C. sylvatica*, *Nebela tincta*, *Schoenbornia humicola*, *Corythion dubium*, *C. dubium* v. *orbicularis*, *Difflugiella minuta*, and *Pseudodifflugia gracilis* v. *terricola*. From 136 to 487 specimens were counted per sample and up to 14 species were found per horizon (Fig. 7; Table 2). Modified after Chardez (1965), ecological groups of xerophilic, hygro-hydrophilic, sphagnobiontic, and soil-eurybiontic species were distinguished (Fig. 7). Soil-eurybiontic species can tolerate a wide range of a particular environmental factor; the specific factor (moisture, pH, etc.) varies between species. They are represented by 14 species whose percentage of the whole assemblage decreases from polygon rim to center (Fig. 7). The most abundant soil-eurybiontic

Table 2 Total counts of testate amoeba species in polygon KYT-1 pits

Species	Ecological preference	Abbreviation	Pit 1 (rim)				Pit 2 (inner slope)			
			S	Oi	Oe	Bg	S	Oi	Oe	Bg
Centropyxis aerophila	eury	CenAer	0	0	0	0	0	0	0	0
C. aerophila v. *sphagnicola*	eury	CenAerSph	0	0	0	0	0	0	0	0
C. constricta	eury	CenCon	0	0	0	0	0	3	0	0
C. constricta v. *minima*	eury	CenConMin	0	4	3	0	0	0	0	0
C. ecornis	sphagno	CenEco	0	0	0	0	0	0	0	0
C. platystoma	hydro	CenPla	0	0	0	0	0	0	0	0
C. sylvatica	eury	CenSyl	3	3	21	0	0	0	0	0
Cyclopyxis eurystoma	eury	CycEur	89	5	11	0	78	15	6	0
Heleopera petricola	sphagno	HelPet	0	0	0	0	0	0	0	0
Hyalosphenia papilio	sphagno	HyaPap	0	0	0	0	0	0	0	0
Nebela tincta	sphagno	NebTin	38	0	0	0	0	6	4	0
Schoenbornia humicola	eury	SchHum	0	0	15	0	0	21	8	0
Sch. viscicula	eury	SchVis	0	0	0	0	0	0	0	0
Difflugia gassowski	hydro	DifGas	0	0	0	0	0	0	0	0
D. globulus	hydro	DifGlo	0	0	0	0	0	0	0	0
D. lacustris	hydro	DifLac	0	0	0	0	0	0	0	0
D. minuta	hydro	DifMin	0	0	0	0	0	0	0	0
D. penardi	hydro	DifPen	0	0	0	0	0	0	0	0
Lagenodifflugia vas	hydro	LagVas	0	0	0	0	0	0	0	0
Valkanovia elegans	sphagno	ValEle	0	3	0	0	0	5	0	0
Assulina muscorum	sphagno	AssMus	19	0	0	0	89	0	5	0
Euglypha cristata	sphagno	EugCri	0	0	0	0	0	0	0	0
E. laevis	eury	EugLae	0	0	0	0	0	0	0	0
Placocista spinosa	sphagno	PlaSpi	0	0	0	0	0	0	0	0
Corythion dubium	xero	CorDub	5	4	0	0	135	0	4	0
C. dubium v. *orbicularis*	xero	CorDubOrb	0	0	0	0	16	9	0	0
C. pulchellum	xero	CorPul	1	0	0	0	0	0	0	0
Trinema lineare	eury	TriLin	8	302	67	0	69	14	98	0
T. lineare v. *minuscula*	eury	TriLinMin	0	39	6	0	17	0	7	0
T. lineare v. *terricola*	eury	TriLinTer	0	0	14	0	0	0	5	0
T. lineare v. *truncatum*	eury	TriLinTru	0	24	0	0	0	0	0	0
Cryptodifflugia bassini	sphagno	CryBas	0	0	0	0	0	0	0	0
Difflugiella minuta	hydro	DiffMin	0	0	0	0	0	0	0	0
D. oviformis f. *fusca*	eury	DiffOviFus	187	103	0	0	87	247	18	0
Pseudodifflugia gracilis v. *terricola*	sphagno	PseGraTer	0	0	0	0	0	102	34	0
Wailesella eboracensis	sphagno	WaiEbo	0	0	0	0	0	5	0	0
Amphitrema flavum	sphagno	AmpFla	0	0	0	0	0	0	0	0
Number of specimens per sample			350	487	137	0	491	427	189	0
Number of species per sample			8	9	7	0	7	10	10	0
Number of species per pit						14				14
Total number auf species			37							

Species	Pit 3 (center)				Pit 4 (center)			
	S	Oi	Oe	Bg	S	Oi	Oe	Bg
Centropyxis aerophila	0	16	0	0	0	0	4	0
C. aerophila v. *sphagnicola*	0	3	0	0	0	0	0	0
C. constricta	0	7	0	0	0	85	3	0

Table 2 continued

Species	Pit 3 (center)				Pit 4 (center)			
	S	Oi	Oe	Bg	S	Oi	Oe	Bg
C. constricta v. *minima*	0	0	0	0	0	0	0	0
C. ecornis	0	0	5	0	0	0	0	0
C. platystoma	0	0	0	0	0	0	7	0
C. sylvatica	0	9	0	0	0	3	3	0
Cyclopyxis eurystoma	0	0	5	0	0	0	0	0
Heleopera petricola	0	0	0	0	9	0	4	0
Hyalosphenia papilio	0	5	0	0	0	0	0	0
Nebela tincta	0	4	0	0	9	8	0	0
Schoenbornia humicola	0	29	4	0	0	0	3	0
Sch. viscicula	0	0	0	0	0	3	0	0
Difflugia gassowski	0	0	0	0	0	0	3	0
D. globulus	0	0	0	0	0	0	5	0
D. lacustris	0	0	0	0	0	0	2	0
D. minuta	0	0	16	0	0	0	0	0
D. penardi	0	0	0	0	0	0	4	0
Lagenodifflugia vas	0	0	0	0	0	0	1	0
Valkanovia elegans	0	0	0	0	4	4	0	0
Assulina muscorum	139	0	0	0	13	10	0	0
Euglypha cristata	0	0	0	0	4	0	0	0
E. laevis	0	0	0	0	56	0	0	0
Placocista spinosa	0	0	0	0	3	0	0	0
Corythion dubium	24	0	0	0	0	0	0	0
C. dubium v. *orbicularis*	7	0	0	0	0	0	0	0
C. pulchellum	0	0	0	0	0	0	0	0
Trinema lineare	23	135	25	0	7	0	39	0
T. lineare v. *minuscula*	3	6	0	0	0	0	0	0
T. lineare v. *terricola*	0	0	0	0	0	0	0	0
T. lineare v. *truncatum*	0	0	5	0	0	0	0	0
Cryptodifflugia bassini	0	0	0	0	24	0	0	0
Difflugiella minuta	0	0	76	0	0	162	356	3
D. oviformis f. *fusca*	235	9	0	0	54	36	7	0
Pseudodifflugia gracilis v. *terricola*	0	7	0	0	0	0	0	0
Wailesella eboracensis	0	0	0	0	131	0	0	0
Amphitrema flavum	0	0	0	0	3	0	0	0
Number of specimens per sample	431	230	136	0	317	311	441	3
Number of species per sample	6	11	7	0	12	8	14	1
Number of species per pit				19				24
Total number auf species								

Species' ecological preferences are given as soil-eurybiontic (eury), xerophilic (xero), hygro-hydrophilic (hydro), and sphagnobiontic (sphagno)

species in the data set are *Trinema lineare* and *Difflugiella oviformis* f. *fusca*. Other species occurred in much lower numbers. Only three species of the xerophilic group (*Corythion dubium*, *C. dubium* v. *orbicularis*, *C. pulchellum*) were found in the best-drained samples from the inner slope surface (pit 2). Seven hygro-hydrophilic species were only found in subsurface polygon center samples taken from pits 3 and 4. The main representative of the hygro-hydrophilic group is *Difflugia minuta*. Twelve species belong to the sphagnobiontic group; they are mostly present in surface and near-surface samples from the polygon center (pits 3 and 4). Typical species are *Assulina muscorum*, *Nebela tincta,* and *Pseudodifflugia gracilis* v. *terricola*.

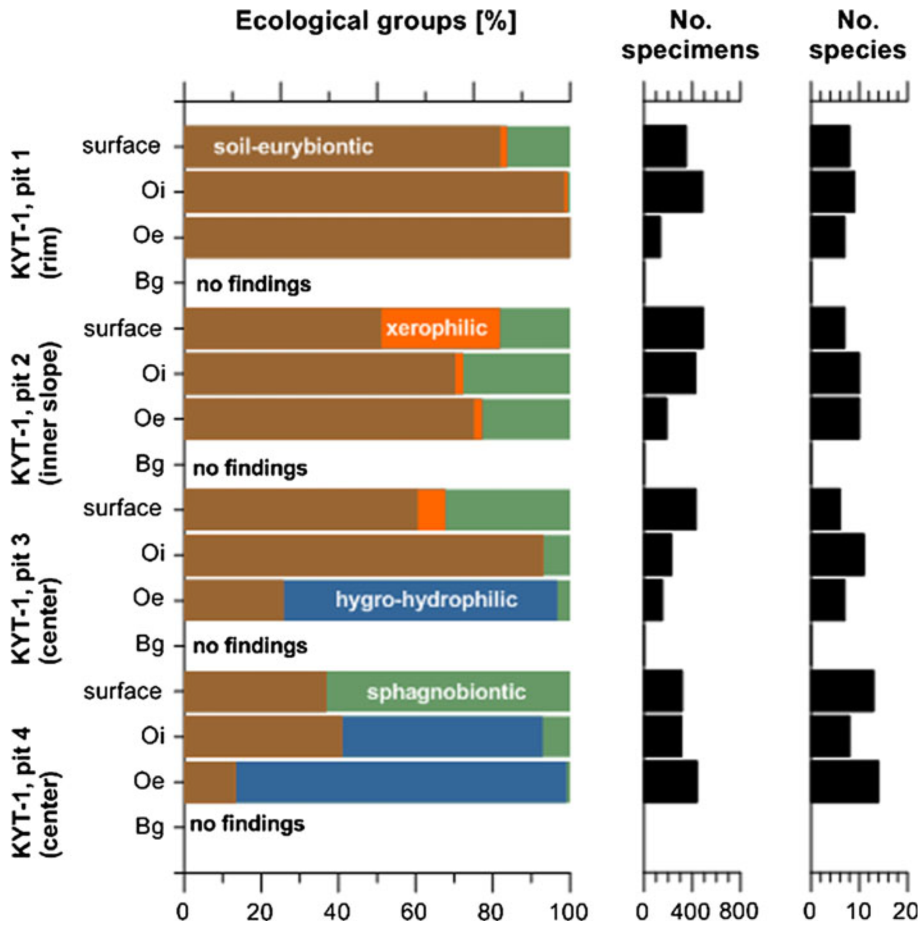

Fig. 7 Distribution of ecological groups of testate amoebae assemblages in different horizons of four pits within polygon KYT-1 (*brown* soil-eurybiontic species, *orange* xerophilic species, *green* sphagnobiontic species, *blue* hygro-hydrophilic species)

On the polygon rim (pit 1), 14 taxa were found (Table 2). The most abundant species belong to the sphagnobiontic and soil-eurybiontic ecological groups and are represented by the genera *Assulina*, *Valkanovia*, *Centropyxis*, *Cyclopyxis*, *Trinema,* and *Difflugiella*. In the surface horizon, high numbers of *Difflugiella oviformis* f. *fusca* and *Cyclopyxis eurystoma* were obtained. The latter decreased in the Oi horizon, while the number of *Trinema lineare* specimens increased. *Trinema lineare* remains were dominant within the Oe horizon, accompanied by high numbers of the eurybiontic species *Centropyxis sylvatica*. Hygro-hydrophilic species were not found. The total number of species found in the inner slope (pit 2) represents 14 taxa including *Cyclopyxis eurystoma*, *Assulina muscorum*, *Corythion dubium*, *Trinema lineare*, *Difflugiella oviformis* f. *fusca*, and *Pseudodifflugia gracilis* v. *terricola* (Table 2). The surface horizon was dominated by *Corythion dubium* and *C. dubium* v. *orbicularis* whose numbers decreased in underlying horizons, while numbers of *Difflugiella oviformis* f. *fusca* and *Pseudodifflugia gracilis* v. *terricola* increased with depth. No hygro-hydrophilic species were found in inner slope samples. In the polygon center (pit 3), 19 species were identified. Most common were *Assulina muscorum*, *Trinema lineare*, *Difflugiella minuta*, and *D. oviformis* f. *fusca*. Occurrence of the hygrophilic species *Centropyxis ecornis* and the hydrophilic species *Difflugia minuta* point to the different moisture conditions as in the polygon rim. A total of 24 species were obtained from the polygon center (pit 4; Table 2). Twelve species were found in the surface horizon. Among them the diversity of sphagnobiontic species is remarkable; species include *Valkanovia elegans*, *Assulina muscorum*, *Euglypha cristata*, *Heleopera petricola*, *Hyalosphenia papilio*, *Nebula tincta*, *Placocista spinosa*, *Difflugiella bassini*, *Pseudodifflugia gracilis* v. *terricola*, *Wailesella eboracensis* and *Amphitrema flavum*. The number of species decreases to 8 in the Oi horizon and increases to 14 in the Oe horizon. Hygro-hydrophilic species of the genera *Centropyxis*, *Difflugia*, and *Lagenodifflugia* dominate the assemblages.

The surface samples of all four studied pits contained 17 species dominated by sphagnobiontic species of the genera *Assulina*, *Heleopera*, *Nebela*, *Valkanovia*, *Corythion*, *Wailesella*, and *Amphitrema*. The most common species are *Assulina muscorum*, *Corythion dubium*, and *Difflugiella oviformis* f. *fusca* (Table 2). The surface horizon lacked hygro-hydrophilic species.

The Oi horizon of all studied pits contained, in total, 21 species; numbers of *Centropyxis constricta* increase from the polygon rim toward its center, while *Trinema lineare* and subspecies disappear (Table 2). The hygro-hydrophilic species *Difflugiella minuta* occurs in high numbers in the Oi horizon of center pit 4. The highest number of species per horizon, 25, is reached within the Oe horizon (Table 2). Here, all ecological groups are present; the increased numbers of the hygro-hydrophilic species *Difflugiella minuta* in pit 4 are remarkable. Except for 3 specimens of *Difflugiella minuta* observed in pit 4, the Bg horizon generally lacks testate amoeba specimens.

A non-metric multidimensional scaling (nMDS) was performed to explore the relationships between samples and species composition in the testate amoeba data set. The run-on two-dimensional space produced a stress value of 11.5 %, indicating a good fit between the original distance of objects and the fitted values. Figure 6 illustrates the nMDS ordination results based on Bray-Curtis distances in a biplot. The plot shows the differences between the pits; it also indicates that the species assemblages in different soil horizons are somewhat similar. Taxa grouping on the upper left side of the plot are predominantly sphagnobiontic taxa, while hygro-hydrophilic taxa are located on the upper right side, and xerophilic taxa on the lower left side. In comparison with the other ecological groups, soil-eurybiontic taxa are scattered more widely throughout the plot. Pedochemical properties and location parameters ("distance-to-rim", depth, horizon) were added to supplement the nMDS plot. The length of the arrows in Fig. 6 is proportional to the strength of the relationship between the testate amoeba data and the pedochemical properties or location parameters. Location and pH show the strongest relationship with the data set.

Discussion

The micro-relief of the studied KYT-1 polygon and the corresponding differentiation of environmental parameters control the distribution of testate amoeba species. Generally, the polygon rim is characterized by drier conditions than are found in the polygon center due to its relatively higher position with better drainage. The higher water content of the polygon center causes a deeper seasonally thawed active layer to develop because free water in the soil has higher thermal conductance than the organic and mineral soil components. As a result, the deeper-lying permafrost table of the polygon center enables higher ground temperatures. The surface vegetation delineates the moisture conditions within the polygon by, for example, the occurrence of dwarf shrubs on the dry rim and sedges and semiaquatic herbs, for example, Marsh Cinquefoil (*Potentilla palustris*), in the wet center.

The pedochemical data obtained from different soil horizons along the studied transect differ with depth rather than with position in the polygon. Generally, as indicated by soil sample measurements, the water content in all pits decreases toward the permafrost table (Table S2). The water content in surface samples was not measured (Fig. 5), but it seems reasonable to assume that the content varies depending upon rainfall events (Fig. 4). The highest soil moisture values of the monitoring data set (Fig. 4) were measured at a depth of 27 cm within the Oe horizon, and the lowest soil moisture values were measured at a depth of 12 cm. This is probably due to the position of the sensors within the inner slope, where drainage through the uppermost horizons toward the polygon center is likely. The two approaches used to quantify the moisture regime are not directly comparable, but both data sets indicate that the wettest conditions are found within the Oe horizons and the Bg horizons are drier. The decrease in the water content toward the permafrost table is explained by the change of the substrate. The organic material of the Oi- and Oe horizons can hold much more water than mineral Bg horizons. High organic contents and low pH values are typical for polygonal tundra (e.g., Fiedler et al. 2004). Pore water pH increases with depth, while EC decreases or remains stable. Both observations are again connected to the change of substrate.

The accumulation and decomposition of organic matter is expressed in total carbon and nitrogen contents and in C/N ratios. Decomposition under arctic conditions is a rather slow process because under the influence of the near-surface permafrost table temperatures are low and moisture content is high within the active layer, resulting in a generally low rate of organic matter mineralization. Oi and Oe peat horizons are clearly differentiated from lowermost Bg horizons (Table S2). The low decomposition rate of organic matter is evidenced by rather high C/N ratios. Extractable nitrate and phosphate contents decrease with depth in each pit, while the highest nitrogen and extractable ammonium contents occur in the Oe horizon. There are considerable variations in the amount of available nutrients during the vegetation period in arctic soils (Weintraub and Schimel 2005). As our samples have been taken only on a single date, we have no information about the seasonal variation. But compared to other studies, we find amounts of available nutrients in the normal range of seasonal variation (Chapin et al. 1978; Weintraub and Schimel 2005).

The studied KYT-1 polygon clearly offers differentiated ground temperature, soil moisture, pH, and organic matter conditions along a spatial transect toward the center and/or with depth below surface. The testate amoeba assemblages mainly correspond to the moisture gradient from the rim to the center as reflected by increasing numbers of hygro-hydrophilic species of the genera *Difflugiella*, *Difflugia*, and *Lagenodifflugia* from the rim toward the polygon center. Xerophilic species of the genus *Corythion* occur in considerable numbers only in the well-drained surface sample from the inner slope (Fig. 7; Table 2). The finding of *Corythion* in the surface sample of pit 3 (center) and the absence of hygro-hydrophiles in the surface and the Oi horizon samples indicate a varying water table in this part of the polygon.

Hygro-hydrophiles occur in lower water-saturated Oi and Oe horizons; xerophiles characterize the drier habitats of well-drained horizons. If the ground occasionally dries out, a considerable number of xerophiles may be established, as was found in the surface horizon of pit 2 (inner slope). The strong relationship between the location within the polygon and species distribution (Fig. 6) supports this conclusion. Studying the spatial distribution of testacean communities in different soil horizons along micro-relief structures (i.e., rim vs. center) by applying a transect and soil profile approach best reflects the controls over habitat conditions and species distribution in polygon tundra landscapes. The other main control over species distribution is pH (Fig. 6) which increases from the surface toward the permafrost table in each pit, as well as from the rim to the center (Fig. 4). Accordingly, acidophilic species dominate in the rim and the inner slope of the polygon.

The influence of the permafrost table on testacean communities is of special interest. In tundra zone cryosols, the near-surface permafrost table is the primary controller of the ground-water regime. Therefore, the traditional approach in testate amoeba analysis based on estimations of ecological optima and tolerances in relation to the ground-water table seems less applicable for high latitudes because it was established for the oligotrophic *Sphagnum*-dominated wetlands of boreal latitudes (Charman 1997; Bobrov et al. 1999; Mitchell and Gilbert 2004).

Most of the identified species at the Kytalyk study site are cosmopolitans and therefore not indicative of the specific arctic environment of the polygonal tundra. Modern testacean associations in Arctic Siberia have so far been described only from western and central parts (Beyens et al. 2000), while intense work has been done in northern Sweden (Tsyganov et al. 2012), in Greenland (Beyens et al. 1992; Trappeniers et al. 1999; Mattheeussen et al. 2005; Beyens et al. 2009; Tsyganov et al. 2011), in Alaska (Payne et al. 2006; Markel et al. 2010), and in Canada (Beyens et al. 1990). Beyens et al. (1986a, b) and Beyens and Chardez (1995) conducted overview studies on arctic testacean assemblages from Alaska, Canada, East Greenland, Jan Mayen Island, and northwestern and central Spitsbergen. Eight species found in the Kytalyk study site are described for the first time from the Arctic: *Amphitrema flavum*, *Difflugia gassowski*, *Difflugiella (Cryptodifflugia) bassini*, *Lagenodifflugia vas*, *Schoenbornia humicola*, *Sch. viscicula*, *Valkanovia elegans*, and *Wailesella eboracensis*.

Conclusions

The main goal of the study was to gauge the variability of testate amoeba communities along vertical (profile) and horizontal (rim to center) gradients of polygon micro-relief. The polygon-specific setting (i.e., moisture regime, ground temperature, and pedochemistry) was analyzed in order to relate the environmental conditions to testacean species distribution. Such research is useful for interpreting fossil communities from polygon deposits.

The following conclusions can be drawn: (1) Environmental parameters that affect testate amoeba communities in arctic polygon tundra vary within the studied polygon from the rim toward the center and/or with depth; (2) the most important controls on testacean species distribution are the moisture regime, which varied according to position within the studied polygon, and pH; (3) the number of species increases from the polygon rim toward the center where warmer and wetter conditions prevail in a seasonally deeper thawed active layer; (4) along the rim-to-center gradient soil-eurybiontics and xerophiles are replaced by sphagnophiles in surface samples, and soil-eurybiontic species are replaced by hygro-hydrophiles in lower Oi and Oe soil horizons; (5) using the ecological indication of testacean taxa, increasing soil moisture can be only observed for the Oi and Oe horizons; and (6) lowermost (and coldest) Bg horizons directly above the permafrost table lack testaceans.

Acknowledgments The study was conducted under the auspices of the joint Russian–German project “Polygons in tundra wetlands: State and dynamics under climate variability in polar regions” (Russian Foundation for Basic Research, RFBR Grant No. 11-04-91332-NNIO-a, Deutsche Forschungsgemeinschaft, DFG Grant No. HE 3622-16-1). Financial support came also from the RFBR Project No. 11-04-01171-a “Geography and ecology of soil-inhabiting testate amoebae”. Our field studies in Kytalyk were realized in coordination with Dutch groups from the Vrije Universiteit Amsterdam (led by Ko van Huissteden) and the University of Wageningen (led by Monique Heijmans). Finally, we would like to thank the Committee of Nature Conservation in Chokurdakh (Evgeny Yanyigin, Tatyana Gavrilova) for logistical support. The manuscript preparation and revision greatly benefited by valuable comments and English language correction from Candace O’Connor (University of Alaska, Fairbanks).

References

Andreev A, Grosse G, Schirrmeister L, Kuznetsova T, Kuzmina S, Bobrov A, Tarasov P, Novenko E, Meyer H, Derevyagin A, Kienast F, Bryantseva A, Kunitsky V (2009) Weichselian and Holocene palaeoenvironmental history of the Bol’shoy Lyakhovsky Island, New Siberian Archipelago, Arctic Siberia. Boreas 38:72–110. doi:10.1111/j.1502-3885.2008.00039.x

Beyens L, Chardez D (1995) An annotated list of testate amoebae observed in the Arctic between the longitudes 27° E and 168° W. Arch Protistenkd 146:219–233. doi:10.1016/S0003-9365(11)80114-4

Beyens L, Chardez D, Baere D, with collaboration of de Bock P (1992) The testate amoebae from the Søndre Strømfjord region (West-Greenland): their biogeographic implications. Arch Protistenkd 142:5–13. doi:10.1016/S0003-9365(11)80092-8

Beyens L, Chardez D, de Baere D, with collaboration of de Bock P, Jacques E (1990) Ecology of terrestrial testate amoebae assemblages from coastal lowlands on Devon Island (NWT, Canadian Arctic). Polar Biol 10:431–440. doi:10.1007/BF00233691

Beyens L, Chardez D, de Landtsheer R, with collaboration of de Baere D (1986a) Testate amoebae communities from aquatic habitats in the Arctic. Polar Biol 6:197–205. doi:10.1007/BF00443396

Beyens L, Chardez D, de Landtsheer R, with collaboration of de Bock P, Jacques E (1986b) Testate amoebae populations from moss and lichen habitats in the Arctic. Polar Biol 5:165–173. doi:10.1007/BF00441696

CAVM Team (2003) Circumpolar Arctic vegetation map. Conservation of Arctic Flora and Fauna (CAFF) Map No. 1. US Fish and Wildlife Service, Anchorage, Alaska

Beyens L, Chardez D, van de Vijver BA (2000) Contribution to the protist-diversity in the polar regions: testate amoebae data from the Russian Arctic. In: Ceulemans R, Bogaert J, Deckmyn G, Nijs I (eds) Topics in ecology. Structure and function in plants and ecosystems. University of Antwerpen, UIA, Wilrijk, pp 101–110

Beyens L, Ledeganck P, Graae BJ, Nijs I (2009) Are soil biota buffered against climatic extremes? An experimental test on testate amoebae in arctic tundra (Qeqertarsuaq, West Greenland). Polar Biol 32:453–462. doi:10.1007/s00300-008-0540-y

Bobrov AA, Charman DJ, Warner BG (1999) Ecology of testate amoebae (Protozoa: Rhizopoda) on peatlands in Western Russia with special attention to niche separation in closely related taxa. Protist 150:125–136. doi:10.1016/S1434-4610(99)70016-7

Bobrov AA, Andreev AA, Schirrmeister L, Siegert C (2004) Testate amoebae (Protozoa: Testacealobosea and Testaceafilosea) as bioindicators in the late quaternary deposits of the Bykovsky Peninsula, Laptev Sea, Russia. Palaeogeogr Palaeoclimatol Palaeoecol 209:165–181. doi:10.1016/j.palaeo.2004.02.012

Bobrov A, Müller S, Chizhikova N, Schirrmeister L, Andreev A (2009) Testate amoebae in late quaternary sediments of the Cape Mamontov Klyk (Yakutia). Biol Bull 36:363–372. doi:10.1134/S1062359009040074

Bowman RA, Cole CV (1978) An exploration method for fractionation of organic phosphorus from grassland soils. Soil Sci 125:95–101

Chapin FS III, Barsdate RJ, Barèl D (1978) Phosphorus cycling in Alaskan coastal tundra: a hypothesis for the regulation of nutrient cycling. Oikos 31:189–199

Chardez D (1965) Ecologie générale des Thécamoebiens. Bull Inst Agron Stn Rech Gembloux 33:307–341

Charman DJ (1997) Modelling hydrological relationships of testate amoebae (Protozoa: Rhizopoda) on New Zealand peatlands. J R Soc N Z 27:465–483. doi:10.1080/03014223.1997.9517549

Charman DJ (2001) Biostratigraphic and palaeoenvironmental applications of testate amoebae. Quat Sci Rev 20:1753–1764. doi:10.1016/S0277-3791(01)00036-1

Charman DJ, Blundell A, Members A (2007) A new European testate amoebae transfer function for palaeohydrological reconstruction on ombrotrophic peatlands. J Quat Sci 22:209–221. doi:10.1002/jqs.1026

DIN (1996) DIN ISO 10694. Soil quality—determination of organic and total carbon after dry combustion (elementary analysis). Beuth, Berlin

Fiedler S, Wagner D, Kutzbach L, Pfeiffer E-M (2004) Element redistribution along hydraulic and redox gradients of low-centered polygons, Lena Delta, Northern Siberia. Soil Sci Soc Am J 68:1002–1011. doi:10.2136/sssaj2004.1002

Geocryological Map (1991) Geocryological Map of the USSR, scale 1:2,500,000. Yershov ED (ed) Moscow State University, Faculty of Geology, Department of Geocryology (in Russian)

Gilbert D, Amblard C, Bourdier G, Francez AJ (1998) The microbial loop at the surface of a peatland: structure, function, and impact of nutrient input. Microb Ecol 35:83–93. doi:10.1007/s002489900062

Ivanoff DB, Reddy KR, Robinson S (1998) Chemical fractionation of organic phosphorus in selected histosols. Soil Sci 163:36–45

Lamarre A, Garneau M, Asnong H (2012) Holocene paleohydrological reconstruction and carbon accumulation of a permafrost peatland using testate amoeba and macrofossil analyses, Kuujjuarapik, subarctic Québec, Canada. Rev Palaeobot Palynol 186:131–141. doi:10.1016/j.revpalbo.2012.04.009

Markel E, Booth RK, Qin Y (2010) Testate amoebae and δ^{13}C of *Sphagnum* as surface moisture proxies in Alaskan peatlands. Holocene 20:463–475. doi:10.1177/0959683609354303

Mattheeussen R, Ledeganck P, Vincke S, van de Vijver B, Nijs I, Beyens L (2005) Habitat selection of aquatic testate amoebae communities on Qeqertarsuaq (Disko Island), West Greenland. Acta Protozool 44:253–263

Meyer H, Schirrmeister L, Andreev A, Wagner D, Hubberten H-W, Yoshikawa K, Bobrov A, Wetterich S, Opel T, Kandiano E, Brown J (2010) Late Glacial and Holocene isotopic and environmental history of Northern Alaska—results from a buried ice-wedge system at Barrow. Quat Sci Rev 29:3720–3735. doi:10.1016/j.quascirev.2010.08.005

Mitchell EAD, Gilbert D (2004) Vertical micro-distribution and response to nitrogen deposition of testate amoebae in *Sphagnum*. J Eukaryot Microbiol 51:480–490. doi:10.1111/j.1550-7408.2004.tb00400.x

Mitchell EAD, Charman DJ, Warner BG (2008) Testate amoebae analysis in ecological and paleoecological studies of wetlands: past, present and future. Biodivers Conserv 17:2115–2137. doi:10.1007/s10531-007-9221-3

Müller S, Bobrov A, Schirrmeister L, Andreev A, Tarasov PE (2009) Testate amoebae record from the Laptev Sea coast and its implication for the reconstruction of Late Pleistocene and Holocene environments in the Arctic Siberia. Palaeogeogr Palaeoclimatol Palaeoecol 271:301–315. doi:10.1016/j.palaeo.2008.11.003

Oksanen J, Kindt R, Legendre P, O'Hara B, Simpson GL, Solymos P, Stevens MHH, Wagner H (2008) Vegan: community ecology package. R package version 1.15-1

Payne RJ, Kishaba K, Blackford JJ, Mitchell EAD (2006) Ecology of testate amoebae (Protista) in south-central Alaska peatlands: building transfer-function models for palaeoenvironmental studies. Holocene 16:403–414. doi:10.1191/0959683606hl936rp

Payne RJ, Mitchell EAD, Nguyen-Viet H, Gilbert D (2012) Can pollution bias peatland paleoclimate reconstruction? Quat Res 78:170–173. doi:10.1016/j.yqres.2012.05.004

Pitulko VV (2011) The Berelekh quest: a review of forty years of research in the mammoth graveyard in northeast Siberia. Geoarchaeol 26:5–32. doi:10.1002/gea.20342

R Development Core Team (2008) A language and environment for statistical computing. R Foundation for Statistical Computing, Vienna

Reichelt G, Willmanns O (1973) Vegetationsgeographie. G. Westermann, Braunschweig

Rivas-Martínez S (1996-2009) Climate diagrams. Worldwide bioclimatic classification system. Phytosociological Research Center, Spain, online source: www.globalbioclimatics.org. Assessed 01 March 2011

Schirrmeister L, Grosse G, Schnelle M, Fuchs M, Ulrich M, Kunitsky V, Grigoriev M, Andreev A, Kienast F, Meyer H, Babiy O, Klimova I, Bobrov A, Wetterich S, Schwamborn G (2011) Late quaternary paleoenvironmental records from the western Lena Delta, Arctic Siberia. Palaeogeogr Palaeoclimatol Palaeoecol 299:175–196. doi:10.1016/j.palaeo.2010.10.045

Schirrmeister L, Pestryakova L, Wetterich S, Tumskoy V (2012) Joint Russian-German polygon project: East Siberia 2011–2014. The expedition Kytalyk 2011. Ber Polarforsch Meeresforsch 653:1–153

Shishov LL, Tonkonogov VD, Lebedeva II, Gerasimova MI (2004) Classification and diagnostics of soils of Russia. Oecumene, Moscow (in Russian)

Soil Survey Staff (2010) Keys to soil taxonomy, 10th edn. US Department of Agriculture & Natural Resources Conservation Service, Washington

Trappeniers K, van Kerckvoord A, Chardez D, Nijs I, Beyens L (1999) Ecology of testate amoebae communities from aquatic habitats in the Zackenberg area (Northeast Greenland). Polar Biol 22:271–278. doi:10.1007/s003000050420

Tsyganov AN, Nijs I, Beyens L (2011) Does climate warming stimulate or inhibit soil protist communities? A test on testate amoebae in high-arctic tundra with free-air temperature increase. Protist 162:237–248. doi:10.1016/j.protis.2010.04.006

Tsyganov AN, Aerts R, Nijs I, Cornelissen JHC, Beyens L (2012) *Sphagnum*-dwelling testate amoebae in subarctic bogs are more sensitive to soil warming in the growing season than in winter: the results of eight-year field climate manipulations. Protist 163:400–414. doi:10.1016/j.protis.2011.07.005

VDLUFA (1991) Methodenbuch 1. Verband Deutscher Landwirtschaftlicher Untersuchungs- und Forschungsanstalten, Darmstadt

Vincke S, Van de Vijver B, Nijs I, Beyens L (2006) Changes in the testacean community structure along small soil profiles. Acta Protozool 45:395–406

Weintraub MN, Schimel JP (2005) The seasonal dynamics of amino acids and other nutrients in Alaskan Arctic tundra soils. Biogeochem 73:359–380. doi:10.1007/sl0533-004-0363-z

Wetterich S, Grosse G, Schirrmeister L, Andreev AA, Bobrov AA, Kienast F, Bigelow NH, Edwards ME (2012) Late quaternary environmental and landscape dynamics revealed by a pingo sequence on the northern Seward Peninsula, Alaska. Quat Sci Rev 39:26–44. doi:10.1016/j.quascirev.2012.01.027

Wilkinson DM, Mitchell EAD (2010) Testate amoebae and nutrient cycling with particular reference to soils. Geomicrobiol J 27:520–533. doi:10.1080/01490451003702925